HNPS Advances in Nuclear Physics

Vol 19 (2011)

HNPS2011

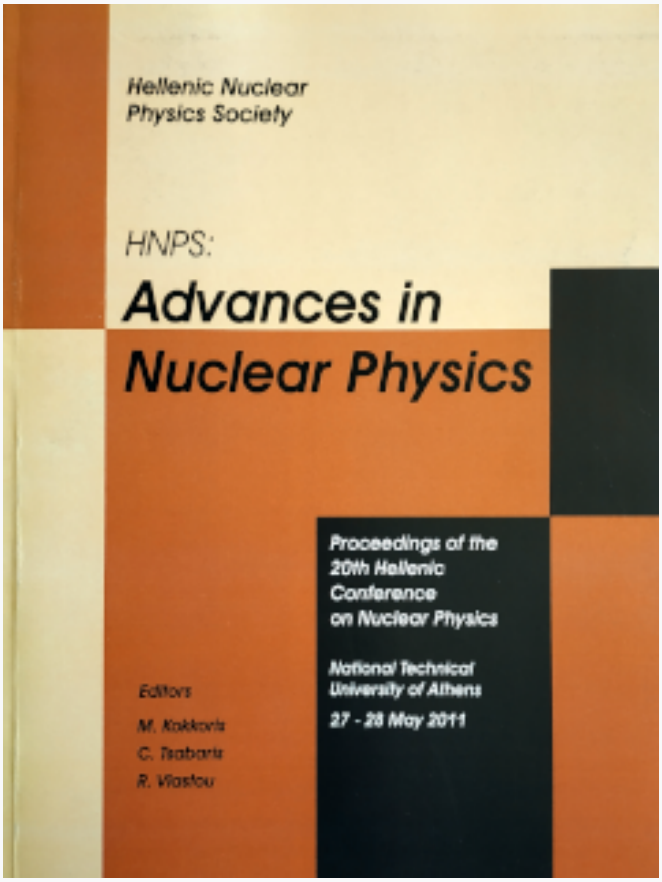

Towards a unification of independent particle and collective models

G. S. Anagnostatos

doi: 10.12681/hnps.2526

Towards a unification of independent particle and collective models

G.S. Anagnostatos

Institute of Nuclear Physics,
National Center for Scientific Research "Demokritos",
Aghia Paraskevi-Attiki, 153 10 Greece

Abstract

A unification of Independent Particle and Collective Models is proposed via the Isomorphic Shell Model. Through this model, based on fundamental properties of fermions, an **average** shape for each nucleus is derived which simultaneously reproduces independent particle and collective properties. ^{20}Ne is taken as an example.

1. Introduction

The Independent Particle Model and the Collective Model are the two fundamental models in nuclear structure theory. Their independent appearances were breakthroughs for their theoretical implications and experimental verifications on different sets of nuclear properties. Very fairly both of them received the highest recognition by the scientific society (Nobel Prize). However, these two basic models have contradicting assumptions. Specifically:

The Independent Particle Model describes the nucleus as a system of **non-interacting** fermions moving in an average potential simulating the effects of all the individual nucleon interactions [1]. The Collective Model describes the nucleus as a system of **strongly** interacting fermions leading to an average shape of the nucleus which may exhibit collective motion like a solid body [1].

Besides the aforementioned obvious contradiction of the models' assumptions, in addition, the assumptions themselves bypass questions concerning basic knowledge of Nuclear Physics: How could someone conceptualize non-interacting particles in a strongly interacting field of force like the nucleus? How could someone compromise the fully quantum mechanical nature of a nucleus with a solid structure of this nucleus?

The purpose of the present work, in the framework of the Isomorphic Shell Model, is to show that **all** successes of the aforementioned contradicting assumptions could be obtained by employing more fundamental physics.

As a demonstration of this achievement the nucleus ^{20}Ne is employed as an example.. This nucleus is in the middle of two doubly closed-shell nuclei, namely ^{4}He and ^{40}Ca, and thus it possesses a large number of low-lying levels. In particular, many low lying 0^{+} levels of this nucleus have been interpreted as band heads of rotational bands in many previous investigations {see references in [2]}. Also, the α-like structure of ^{20}Ne makes its choice even more attractive since it provides a comparison of the present results with those of the α-structure model of a nucleus as well as with those of the aforementioned other two models.

Furthermore, for support of our arguments, an already published work [2] is here utilized in order to avoid ambiguities of the numerical values employed, since the reader can consult the relevant reference for more details of any time.

2. Theoretical part

2.1. The Isomorphic Shell Model

As known, the anti-symmetric wave function of a nucleus has a distribution of its maxima identical to those for repulsive classical particles [3], e.g., on a sphere like the spherical shape of a closed nuclear shell.

This identity shifts the nuclear many-body problem to that of finding the maxima of probability for repulsive particles on a sphere, i.e., of finding their equilibrium positions. In general, such equilibrium positions depend on the law of force among the particles.

Since nuclear forces are very complex and not very well known, we will search for special **equilibria valid for any law of force** (as long as this force depends only on distances between particles). After finding these equilibria we will test if the above requirement is stronger than it should be.

This problem was solved in 1957 by J. Leech [4]: We obtain equilibria independent of the law of force, if in relation to regular polyhedra the repulsive particles are assumed at the vertices, or at the middles of faces, or at the middles of edges, or at any combination of these points.

In testing the above equilibria with respect to fundamental nuclear structure properties, we remark **that** the cumulative numbers of vertices of such properly superimposed polyhedra **precisely** reproduce the magic numbers [5] and **that** taking a proper quantization axis, common for all superimposed polyhedra, we obtain angles, between this axis and the vertices of the polyhedra employed, **identical** to the angles [6-9]:

$$\cos^{-1} m/\sqrt{\ell(\ell+1)}\,, \qquad (1)$$

where ℓ is the orbital angular momentum quantum number and m is the quantum number of its projection on the quantization axis.

Hence, orbital angular momentum is **identically** inherent to the chosen equilibrium polyhedra which when superimposed, in addition, reproduce the magic numbers without considering strong spin-orbit interaction as usual [5]. Thus, our tests for employing equilibrium polyhedra in our approach are successfully satisfied and, of course, the final test will be the comparison of the present results with the experimental data.

The pictorial part of the model is demonstrated in Fig.1 for nuclei with $Z \leq 20$ and $N \leq 20$, where the polyhedra employed are shown in their relative orientation and their average sizes. Their relative orientation is guided by the condition of Eq.(1) and their average sizes are obtained by packing of the relevant polyhedra themselves. That is, this packing is obtained when the bags (r_p = 0.860 fm for protons and r_n = 0.974 fm for neutrons) at the vertices of one polyhedron are in contact with the bags at the vertices of a previous polyhedron [5].

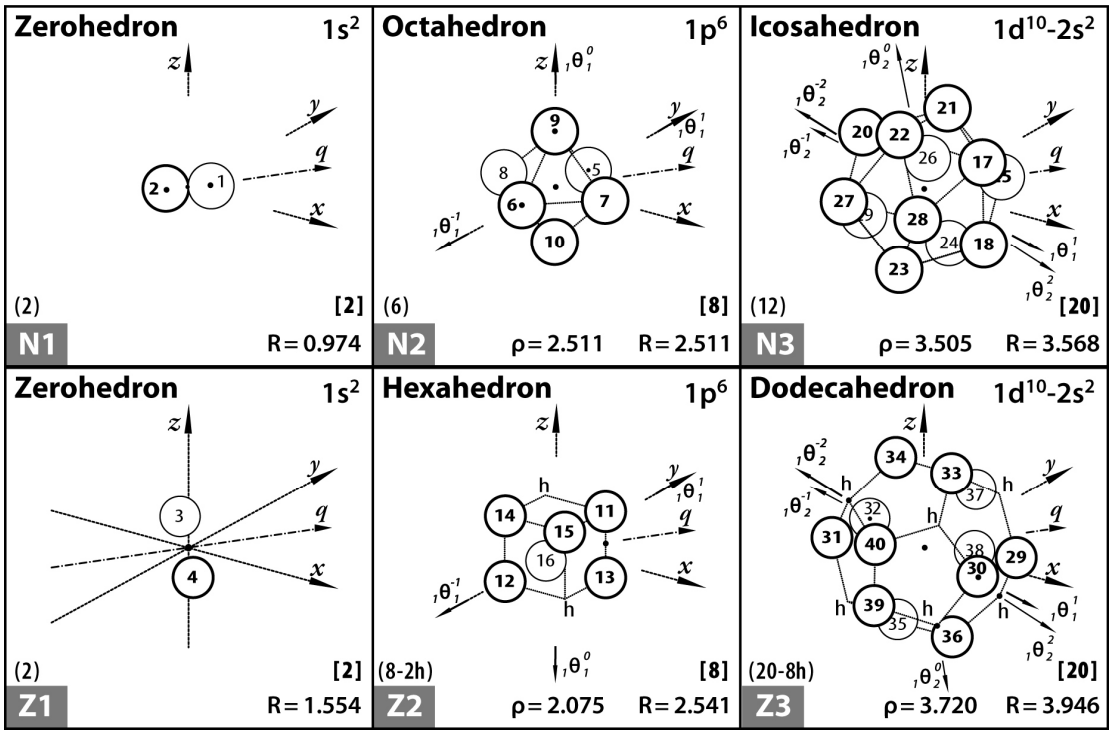

Figure1. The Isomorphic Shell Model for the nuclei up to N=20 and Z=20. The high-symmetry polyhedra in row 1 (i.e., the zerohedron, the octahedron, and the icosahedron) stand for the average forms and sizes of (a) the 1s, (c), the 1p, and (e) the 1d2s shells for neutrons, while the high-symmetry polyhedra in row 2 [i.e., the zerohedron, the hexahedron, (cube), and the dodecahedron] stand for the average forms and sizes of (b) the 1s, (d) the 1p, and (f) the 1d2s shells for protons. The vertices of polyhedra stand for the average positions of nucleons in definite quantum states (τ, n, ℓ , m, s). The letters h stand for the empty vertices (holes), if they exist. The z axis is common for all polyhedra when these are superimposed with a common center and with relative orientation as shown. At the bottom of each block the radius R of the sphere exscribed to the relevant polyhedron and the radius ρ of the relevant classical orbit, equal to the maximum distance of the vertex state (τ, n, ℓ , m, s) from the axis ${}_{n}\theta_{\ell}^{m}$ representing precisely the orbital angular –momentum axis with definite n, ℓ , and m values, are given. All polyhedral vertices are numbered as shown. The backside (hidden) vertices of the polyhedra and the related numbers are not shown in the figure.

2.2. Ehrenfest's theorem.

The Ehrenfest's theorem [10-11] for the observables of position (**R**) and momentum (**P**) takes the form.

$$d\langle \mathbf{R} \rangle/dt = (1/m)\langle \mathbf{P} \rangle \qquad (2)$$

and

$$d\langle \mathbf{P} \rangle/dt = - \langle \nabla V(\mathbf{R}) \rangle . \qquad (3)$$

For simplicity here, the case of a spinless particle in a scalar stationary potential $V(\mathbf{r})$ is considered.

The quantity $\langle \mathbf{R} \rangle$ represents a set of three time-dependent numbers {<X>, <Y>, <Z>} and the point $\langle \mathbf{R} \rangle(t)$ is the center of the wave function at the instant t. The set

of those points which correspond to the various values of t constitutes the trajectory followed by the center of the wave packet.

From Eqs. (1) and (2) we get

$$m d^2\langle \mathbf{R} \rangle / dt^2 = - \langle \nabla V(\mathbf{R}) \rangle . \quad (4)$$

Furthermore, it is known [30] that for special cases of force, e.g., for the harmonic oscillator potential assumed by the Isomorphic Shell Model, the following relationship is valid:

$$\langle \nabla V(\mathbf{R}) \rangle = [\nabla V(\mathbf{r})]_{\mathbf{r} = \langle \mathbf{R} \rangle} , \text{ where} \quad (5)$$

$$-[\nabla V(\mathbf{r})]_{\mathbf{r} = \langle \mathbf{R} \rangle} = \mathbf{F} . \quad (6)$$

That is, for this potential the average of the force over the whole wave function is rigorously equal to the classical force F at the point where the center of the wave function is situated. Thus, for the special case (harmonic oscillator) considered, **the motion of the center of the wave function obeys the laws of classical mechanics**. Any difference between the quantum and the classical description of the nucleon motion depends exclusively on the degree the wave function may be approximated by its center. Such differences will contribute to the magnitude of deviations between the experimental data and the predictions of the semiclassical part of the model employed here.

Now, in the semiclassical treatment the nuclear problem is reduced to that of studying the centers of the wave functions presenting the constituent nucleons or, in other words, of studying the average positions of these nucleons.

Here, the semiclassical part of the model, which has been used many times [2, 12-13] in place of the quantum mechanical part of the model [14] (in the spirit of the above Ehrenfest theorem) is employed. This part of the model is also closer to the α-cluster model [15] and thus a comparison between that model and the present model can be obtained simultaneously with the main purpose of this work aiming towards a unification of Independent Particle and Collective Models.

2.3. Equations of the Isomorphic Shell Model [2]

- $V_{ij}=1.7*10^{17}*e^{-31.8538r_{ij}} /r_{ij}-187*e^{-1.3538r_{ij}}/r_{ij}$ (7)
- $\langle T \rangle_{n \ell m}= (\hbar^2/2M)[1/R^2_{max}+\ell(\ell+1)/\rho^2_{n\ell m}]$ (8)
- $(E_{so})_i = - (20 \pm 5)A^{-2/3}\boldsymbol{\ell}_i.\mathbf{s}_i$ (9)
- $(E_C)_{ij} = e^2/r_{ij}$ (10)
- $E_R=(\hbar^2/2M)I(I+1)/2\square$ (11)
- $E_B.= - \Sigma_{ij}V_{ij} - \Sigma_{n\ell m} \langle T \rangle_{n\ell m} - \Sigma_i(E_{so})_i - \Sigma_{ij}(E_C)_{ij} - E_R$ (12)
- $\langle r^2 \rangle_{ch}^{1/2} = [\Sigma_{i=1}^{Z} R_i^2 /Z + (0.8)^2 – (0.116)N/Z]^{1/2}$ (13)

- $e\,Q'_{20} = \Sigma_i\, e\,Q'_{(20)i} = \Sigma^{Z}_{i=1}\, e\,R^{2}_{i}\,(3\cos^2\theta_i - 1)$ (14)

- $B_{(E2)ex} = 4.08*10^{-6}[E_\gamma(MeV)]^{-5}[\tau(sec)]^{-1}*[1 + \alpha_T\}^{-1}$
  $= Q^{2}_{0}*5/(16\pi)$
  $= \beta^{2}_{2}\,[3ZR^{2}_{0}/4\pi]^2$ (15)

The above equations stand for:

- Eq.(7) for the two body potential in the form of two Yukawa functions,
- Eq.(8) for the average kinetic energy for each nucleon taken as the sum of the kinetic energy due to the uncertainty principle and of the kinetic energy due to the orbiting of the nucleon, where R_{max} is the outermost polyhedral radius R plus the relevant average nucleon radius given above, M is the nucleon mass, and $\rho_{n\ell m}$ is the distance of the vertex (nℓm) from the axis ${}_n\theta^{m}_{\ell}$
- Eq.(9) for the spin-orbit interaction where the energy coefficient (20 ± 5=15–25) starts at its lower values for the lower orbital angular momenta and tends more or less smoothly to the larger values for the higher orbital angular momenta.
- Eq.(10) for the Coulomb energy,
- Eq.(11) for the rotational energy with rotational spin I and □ the moment of inertia of the rotating part of the nucleus plus the quantity (0.165)N [15] for the contribution to the moment of inertia coming from the finite size of the N rotating nucleons, and •
- Eq.(12) for the total binding energy.
- Eq.(13) for the rms charge radius, where $(0.8)^2$ and (0.116) are the mean square charge radii of a proton and of a neutron, respectively.
- Eq.(14) for the intrinsic electric quadrupole moment and θ_i is the azimuthal angle of a proton i with respect to the symmetry axis, and
- Eq.(15) for the reduced electric-quadrupole transition probability between the 0^+ ground state and the first 2^+ state in an even-even nucleus which exhibits a rotational spectrum. In this equation E_γ and τ are the excitation energy and the mean life of the first 2^+ state, α_T is the internal conversion coefficient, and β_2 is the deformation parameter which for a spheroid nucleus with semimajor and semiminor axes a and b takes the expression

$$\beta_2 = 1.06\,(a-b)/R_0, \quad (16)$$

where $R_0 = r_0\,A^{1/3}$ is the nuclear average radius.

3. Calculations.

Calculations refer to distributions of nucleons on the available nucleon average positions of Fig.1 by accommodating the states 1s, 1p, and 1d5/2 involved in ^{20}Ne.

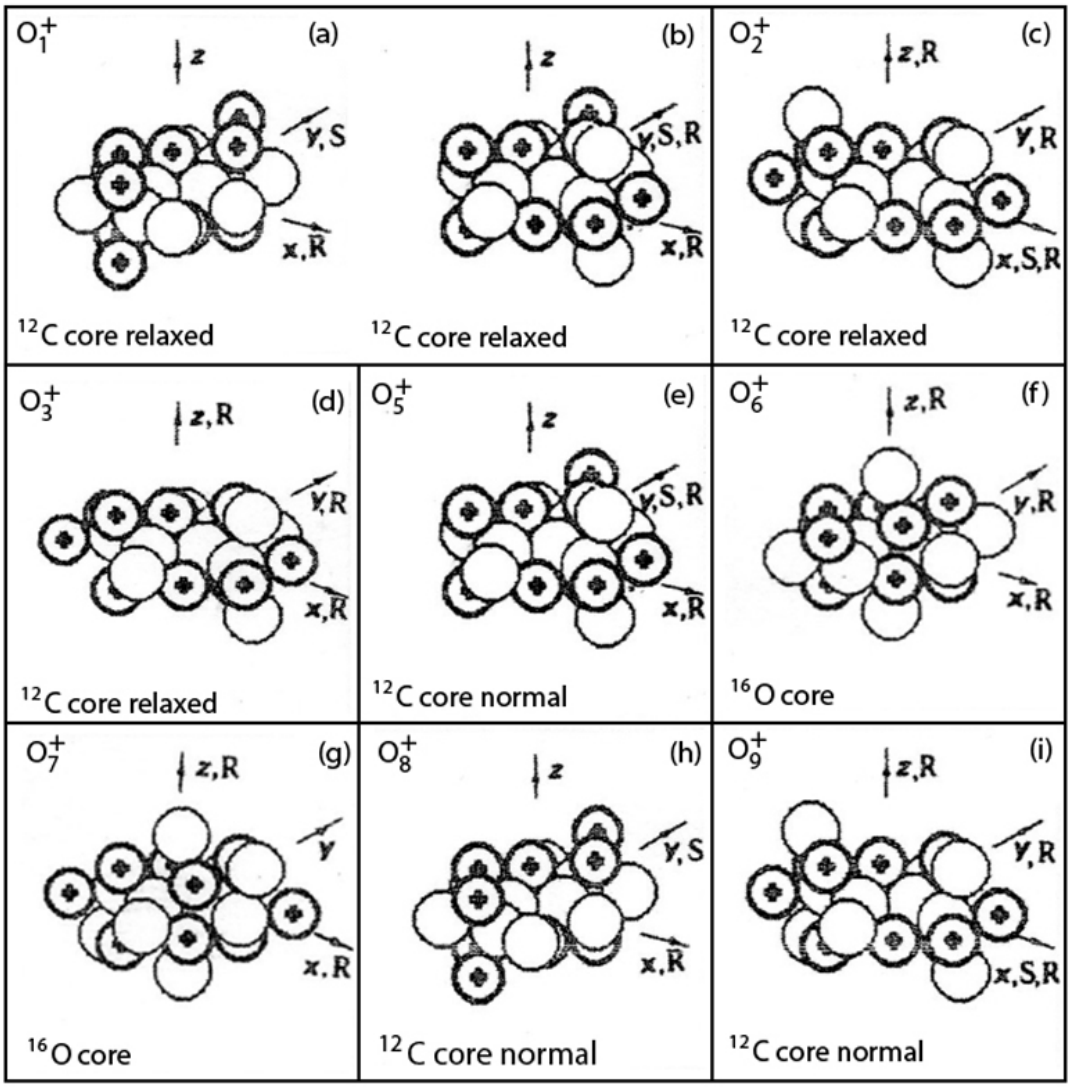

Figure 2. Average forms and sizes for the ground and excited rotational states of ^{20}Ne, according to the Isomorphic Shell Model, composed of the average positions of the constituent nucleons (NAP) numbered as in Fig.1. (a) ^{12}C core relaxed (NAP 1-2, 3_r - 4_r, 5-8, 11-14) plus two α particles on the y axis (NAP 25-26, 37-38, 27-28, 39-40), (b) ^{12}C core relaxed plus one α particle on the x axis and one α particle on the y axis (NAP 17-18, 29-30, 25-26, 37-38), (c) ^{12}C core relaxed plus two α particles on the x axis (NAP 17-18, 29-30, 19-20, 31-32), (d) ^{12}C core relaxed plus one α particle on the x axis (NAP 17-18, 29-30), one pair of neutrons (25-26), and one pair of protons (31-32), (e) ^{12}C core normal (1-8, 11-14) plus one α particle on the x axis and one α particle on the y axis (NAP 17-18, 29-30, 25-26, 37-38), (f) ^{16}O core (NAP 1-16) plus two pairs of one neutron and of one proton (NAP 25, 38; 27, 40, (g) ^{16}O core plus two different pairs of one neutron and of one proton (NAP 17, 29; 19, 31), (h) ^{12}C core normal plus two α particles on the y axis (NAP 25-26, 37-38, 27-28, 39-40), (i) ^{12}C core normal plus two α particles on the x axis (NAP 17-18, 29-30, 19-20, 31-32). Axes labelled x, y, z stand for the axes of coordinates and those labelled S and R for symmetry and rotation axes, respectively, as used in the calculations. Empty spheres stand for neutrons and spheres with a cross for protons.

Figure 2 shows all necessary average forms of ^{20}Ne to investigate the rotational spectra of the following band heads 0_1^+ - 0_3^+ and 0_5^+ - 0_9^+. The 0_4^+ is not a band head of a rotational spectrum [2]. The nine average structures of Fig.2 are among all possible structures for ^{20}Ne [offered by Fig.1 in accommodating 10 neutron average positions on the neutron polyhedra (first row of Fig.1) and 10 proton average positions on the proton polyhedra (second row of Fig.1)] which satisfy the single particle properties of this nucleus having either ^{12}C or ^{16}O as a core [2].

Here, an α-like particle is formed each time a set of 2 neighbouring proton average positions is close to a set of 2 neighbouring neutron average positions and, in addition, this whole arrangement possesses relative angular momentum equal to zero [2, 12-13]. In this respect, with the exception of the structures of (f) and (g) all others shown in Fig.2 are pure α-structures. In each block of the figure the relevant core, either ^{16}O or ^{12}C, is specified. In the caption of this figure the numbering of nucleon average positions (from Fig.1) involved for the structure shown in each block of the figure is given.

In the blocks of Fig.2 where ^{16}O or ^{12}C-normal is the core, the average positions of the two 1s protons are those shown in Fig.1. However, in the blocks of Fig.2 where ^{12}C-relaxed is the core, the average positions of the two 1s protons are those characterized as relaxed, i.e., 3_r and 4_r (not shown in Fig. 1 with coordinates 3_r: x = -1.006 fm, y = 1.006 fm, z = 0.3737 fm and 4_r: x = 1.006 fm, y = -1.006 fm, z = -0.3737 fm). These relaxed positions result from rotation of 3 and 4 of Fig.1(with coordinates 3: x = -0.897 fm, y = z = 0.897 and 4: x = 0.897 fm, y = z = -0.897 fm) around the nuclear center in such a way that their bags remain in contact with those of 1 and 2 and, in addition, come in contact with those of 5,8 and 6,7, respectively. These relaxation positions exist **only** when the core is ^{12}C and thus the neutron average positions 9 and 10 are empty.

By applying Eqs.(7)-(12) to configurations of all parts of Fig.2 we obtain energies E_B and compare them to each other. The E_B values for the configurations a) and b) are identical and larger than those for c) – (i). We assume that 50% of each of the configurations a) and b) contribute to the g.s. and thus their common E_B value is the model g.s. of ^{20}Ne. The differences of the other E_B values from that of the g.s. are the energies of the excited band heads 0_2^+ - 0_3^+ and 0_5^+ - 0_9^+ {see Table 1 of [2]). The relevant moments of inertia and the derived energies via Eq.(11) over the relevant band head of all eight rotational spectra for $I^\pi = 2^+ - 8^+$ are written in Table 1.
Numbers in parentheses in the table stand for the relevant experimental values [16] for comparisons. The excellent closeness of predicted and experimental values is apparent.

4. Discussion

The model applied, the Isomorphic Shell Model, is based on fundamental properties of fermions and not on ad hoc assumptions. The parameters involved in the model are only five and are **universal**, that is, their numerical values remain the same for all nuclear properties in all nuclei. Namely, these parameters are: Two size parameters (i.e., r_p = 0.860 fm and r_n = 0.974 fm), two potential parameters of the second term of Eq.(7) (i.e., 187 MeV and 1.3538 fm, and one spin-orbit parameter λ = 0.03 in Eq.(9). . The values $1.7*10^{17}$ MeV and 31.8538 fm^{-1} of the first Yukawa term in Eq.(7) practically does not affect the numerical values of E_B. This first term is meaningful only in scattering problems.

The closeness of predicted and experimental values in Table 1 mentioned earlier is not the most important comment one could make on the present results. The values of rotational energies when applying the Collective Model could be close to experimental values as well. The most important comment is the one related to the origin of the moment of inertia □ in Eq.(11). In the collective model the numerical value of this **parameter** is obtained by fitting Eq.(11) to several rotational states of the band. In contrast, in the Isomorphic Shell Model the value of the moment of

Table1. 0^+_n, core, energies of band head and excited states in MeV with $I^\pi = 0^+ - 8^+$, and moments of inertia □ in fm^2.

0^+_n	Core	B.H.	2^+	4^+	6^+	8^+	□
0_1	^{12}C	0.000	***1.63**(1.63)	***4.26**(4.25)	***8.78**(8.78)	***15.88**(15.87)	□$_x$=100.4/61.9
						***11.99**(11.95)	
□$_x$=131.5/61.9							
0_2	^{12}C	6.725	**7.39**(7.42)	**8.92**			□$_x$+ □$_y$=189.54
				10.06(9.99)	**13.72**(13.93)	**18.72**(18.96)	□$_y$ =124.48
					13.05(13.11)	**17.56**(17.30)	□$_y$ =137.74
					12.48(12.58)	**16.59**(16.75	□$_z$ =151.30
0_3	^{12}C	7.191	**7.86**(7.83)	**9.41**	**11.85**(12.14)	**15.78**	□$_x$+ □$_y$=186.9
				9.03(9.03)			□$_x$+ □$_z$=225.0
0_5	^{12}C	10.970	**12.31**(12.33)	**15.43**(15.33)	**20.33**(20.17)	**27.02**(28)	□$_x$ = 93.04
			12.26(12.21)	**15.28**(15.33)	**20.03**(20.03)	**26.50**	□$_y$ = 96.14
0_6	^{16}O	11.558	**12.27**(12.22)	**13.94**(13.97)	**16.55**(16.51)	**20.12**	□$_x$+ □$_y$=174.3
						18.44(18.62)	□$_x$+ □$_z$ =216.8
0_7	^{16}O	12.433	**13.01**(12.96)	**14.35**(14.27)	**16.45**(16.87)	**19.32**(19.73)	□$_x$+ □$_z$=216.8
0_8	^{12}C	13.222	**14.17**(14.12)	**16.37**(16.33)	**19.84**(19.85)	**24.57**(24.9)	□$_x$ =131.54
			13.90(13.91)	**15.48**(15.33)	**17.97**(18.29)	**21.36**	□$_x$+ □$_y$=183.34
0_9	^{12}C	15.820	**16.48**(16.44)	**18.01**(18.08)	**20.41**(20.42)	**23.70**(23.4)	□$_x$+ □$_y$=189.54

* % of participation for 2^+ 0.50a/0.50b, 4^+ 0.95a/0.05b, 6^+ 0.98a/0.02b, 8^+ 0.89a/0.11b in the first row of 0_1, where a= 1.24 and b= 2.01, and for 8^+ 0.95a/0.05b in the second row of 0_1, where a= 11.35 and b= 24.12.

inertia □ is **derived** directly from the average structure of the relevant band head. For our case such structures are shown in Fig.2. Indeed, **the moment of inertia in the Isomorphic Shell Model is not a parameter.**

The ground state structure or that of each band head comes from the search to find which occupations of nucleon average positions in Fig.1 approximate the ground state energy or that of the relevant band head. Apparently, all other independent particle properties should be simultaneously reproduced by the same structures. Such structures are completely defined with respect to the two size parameters r_p and r_n. Indeed, according to these two size parameters, the coordinates of the polyhedral vertices and thus of all nucleon average positions are determined [17]. These

structures themselves are direct consequences of the fermionic nature of nucleons as explained in section 2.1.

Of interest is the fact that rotational branches of the same or different bands of ^{20}Ne have almost the same moment of inertia [2], something which has been observed in the study of nuclei in the well-deformed region and particularly in the cases of nuclei with superdeformation, where the moment of inertia gets its largest possible values in the band. In the present model for the cases of superdeformation all nucleons, or almost all, participate in the collective rotation, like the cases described in [2].

Another interesting feature of the moments of inertia in ^{20}Ne is that different axes of rotation have been employed for different members of the same band following the rule that the new axis should lead to a larger moment of inertia for the same average structure. Such behaviour is familiar from the classical rotation of a rigid body possessing three-axial symmetry.

An additional feature found here is that a collective rotation could take place simultaneously around two perpendicular axes, which is another way of increasing the moment of inertia from branch to branch of the same band.

The moments of inertia of two different branches of a band may differ by the moment of inertia of one or more **complete** (deformed) shells from the outermost to the innermost in the series of shells.

The study of ^{20}Ne [2] strongly supports an α-like particle structure of the ground state and many excited states of this nucleus. However, in a moment later than that depicted in Fig.2, each constituent nucleon of these α-like particles follows its independent particle motion in a well-defined shell model orbital.

In the different parts of Fig.2, the axis of symmetry (S) and the corresponding axis of rotations (R) for each block of the figure are shown. Here, an axis of symmetry can be an axis of rotation as well, since none of these axes of symmetry has the C_∞ symmetry appearing, e.g., in an axially symmetric ellipsoidal.

The Isomorphic Shell Model applied here, which uses the interaction of each individual nucleon with all other nucleons in a nucleus, may provide a lot of information about the intrinsic nuclear structure. Thus, it may contribute towards the microscopic explanation of nuclear properties including excitation mechanisms. Indeed, these subjects are among the most important in the nuclear many-body problem today.

In general, the Isomorphic Shell Model approach has some unique advantages. **Firs**t, it can determine all observables {see Table V of [2]} starting from the proper configuration of the nucleon average positions. This configuration results directly from general well- accepted properties of fermions. **Second**, it uses no adjustable parameters, and **third** it provides information about the intrinsic structure of a nucleus with no reference to the experimental data. Indeed, it is of interest and remains an open question whether physicists can obtain unambiguous information, e.g., on the nuclear shape and its consequences, from the analysis of the experimental data alone via any other model.

4. Conclusions

The Independent Particle Model and the Collective Model were breakthroughs at the time of their appearance. Almost what even is known in nuclear structure today comes from these two milestone models. However, these models employ

contradicting assumptions (non-interacting fermions the one; strongly interacting fermions the other).

The Isomorphic Shell Model could be considered as a successful hybrid of both aforementioned models which, in addition, takes into account the average size of the nucleons. This model is based on fundamental physics, that of the fermionic nature of nucleons. No adjustable ad hoc assumptions are employed in this model.

Finally, it can be stated that the present work points towards a unification of the independent particle and the collective models in the framework of the Isomorphic Shell Model. That is, it starts from Independent Particle concepts of a nucleus which could be derived from a specific **average** shape of this nucleus. It is this shape and its symmetries which reproduce the collective properties of this nucleus without the intervention of any additional assumption, e.g., strong interacting fermions as in the Collective Model.

Dedication

The present work is dedicated to the memory of the late colleagues Pelagios K. Kakanis who is the first author of reference [2] on which this paper is based and which was his last published work. He performed the necessary calculations by pressing the keys of his computer with a stick fixed by a leather ring around his palm and wrist. This 2011 presentation was made while he was still alive in intensive care. I admired him for his clear mind and his abilities in Physics. I admired him for his strong hope and will to get better from his quadriplegic injury due to a car accident some years ago. On his tombstone at the cemetery in Aghia Paraskevi, his wife and son had engraved, as a summary of his life struggle:

Κερδισμένη ζωή
σε πόνου αντοχή,
σε θητεία αγάπης –
το διαβατήριό μου
για την αιωνιότητα…

References

[1] W.F. Hornyak, *Nuclear Structure* (Academic, New York, 1975).
[2] P.K. Kakanis, G.S. Anagnostatos, Phys. Rev. C **54**, 2996 (1996).
[3] C.W. Sherwin, *Introduction to Quantum Mechanics* (Holt Rinehart and Winston, N.Y. 1959, p.205.
[4] J. Leech, Mathematical Gazette **41**, 81 (1957). **Available on request from the author of the present work since it is not easily accessible.**
[5] G.S. Anagnostatos, Int. J. Theor. Phys. **24**, 579 (1985).
[6] G.S. Anagnostatos, Lett. Nuovo Cimento **22**, 507 (1978).
[7] G.S. Anagnostatos, Lett. Nuovo Cimento **28**, 573 (1980).
[8] G.S. Anagnostatos, Lett. Nuovo Cimento **22**, 507 (1978).
[9] G.S. Anagnostatos, J. Giapitzakis, and A. Kyritsis, Lett. Nuovo Cimento **32**, 332 (1981).
[10] E. Merzbacher, *Quantum Mechanics*, John Wiley and Sons, New York, p.42 (1961).
[11] C. Cohen-Tannoudji, B. Diu, F. Laloe, *Quantum Mechanics*, J. Wiley & sons, N.Y., p. 240 (1977).
[12] G.S. Anagnostatos, P. Ginis, and J. Giapitzakis, Phys. Rev. C **58,** 3305 (1998).
[13] G.S. Anagnostatos, Phys. Rev. C **51,** 152 (1995).
[14] G.S. Anagnostatos, Int. J. Mod. Phys. B **22,** 4511 (2008).

[15] D.M. Brink, in *The Alpha-Particle Model of Light Nuclei*, Proc. Int. School of Physics "Enrico Fermi" Course XXXVI, ed. C. Bloch (Academic, New York, 1966).
[16] F. Ajzenberg-Selove, Nucl. Phys**. A475**, 1 (1987).
[17] C.N. Panos and G.S. Anagnostatos, J. Phys. G 8, 1651 (1982).